



Study on Simulation of on-Center Handling Tests

By Xiao-Feng Wang
Tsinghua University

Abstract- This paper describes a simulation of on-center handling test, in which a linear 3 degrees of freedom vehicle handling model and a power integral steering system model are incorporated to calculate the time histories of steering wheel angle, steering wheel torque, and vehicle lateral acceleration. The cross plots of steering wheel angle-lateral acceleration, steering wheel torque-lateral acceleration, steering wheel torque-steering wheel angle, steering work-lateral acceleration, and steering work gradient-lateral acceleration are drawn and all the on-center handling parameters are determined from them. The simulation results are compared with the data presented in the literatures, which indicates that the simulation results are reasonable.

Keywords: *on-center handling test; simulation; vehicle handling model; power steering system model; time history; steering wheel angle; steering wheel torque; lateral acceleration; cross plot.*

GJRE-B Classification: FOR Code: 090202



Strictly as per the compliance and regulations of :



RESEARCH | DIVERSITY | ETHICS

Study on Simulation of on-Center Handling Tests

Xiao-Feng Wang

Abstract- This paper describes a simulation of on-center handling test, in which a linear 3 degrees of freedom vehicle handling model and a power integral steering system model are incorporated to calculate the time histories of steering wheel angle, steering wheel torque, and vehicle lateral acceleration. The cross plots of steering wheel angle-lateral acceleration, steering wheel torque-lateral acceleration, steering wheel torque-steering wheel angle, steering work-lateral acceleration, and steering work gradient-lateral acceleration are drawn and all the on-center handling parameters are determined from them. The simulation results are compared with the data presented in the literatures, which indicates that the simulation results are reasonable.

Keywords: on-center handling test; simulation; vehicle handling model; power steering system model; time history; steering wheel angle; steering wheel torque; lateral acceleration; cross plot.

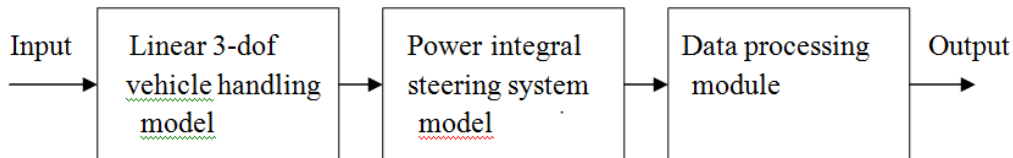
I. INTRODUCTION

Norman (1984) described how to do on-center handling test in detail. On-center handling test has been widely used to measure handling characteristics observed by a car driver during normal highway and freeway driving. It is also one of the essential tests used by car and its steering system manufacturers to quantify the performance of steering systems. The simulation of on-center handling test can help them determine the appropriate system parameters

combination to make a car have good on-center handling characteristics.

There have been some papers published, in which the methods for simulating on-center handling tests are introduced. Post et al. (1996) and Kim (1997) described different simulation methods but they didn't present all the on-center handling cross plots and determine all the on-center handling parameters necessary for characterizing vehicle's on-center handling performance prescribed by Norman (1984).

This paper describes a simulation of on-center handling test, which is based on the test procedure presented by Norman (1984). A linear 3-dof (degrees of freedom) vehicle handling model and a power integral steering system model are incorporated to calculate the time histories of steering wheel angle, steering wheel torque, and vehicle lateral acceleration. The cross plots of steering wheel angle-lateral acceleration, steering wheel torque-lateral acceleration, steering wheel torque-steering wheel angle, steering work-lateral acceleration, and steering work gradient-lateral acceleration are drawn and all the on-center handling parameters are determined from them. Fig.1 shows the main modules of the simulation program.



Input: reference steer angle of vehicle front wheels

Output: on-center handling cross plots and parameters

Fig. 1: Main modules of the simulation program

II. 3-DOF VEHICLE HANDLING MODEL

A linear 3-dof vehicle handling model is adopted in the simulation because the peak lateral acceleration is limited to about 0.2g in the on-center handling tests as prescribed by Norman (1984). This

kind of model can give sufficiently accurate simulation results in such low lateral acceleration range. Fig.2 shows the model. In the model, SAE vehicle and tire axis systems are applied. The three degrees of freedom are

Author: State Key Laboratory of Automotive Safety and Energy, Department of Automotive Engineering, Tsinghua University, Beijing 100084, P. R. China. e-mail: wangxf60@mail.tsinghua.edu.cn

yaw velocity r , sideslip angle β , and roll angle ϕ . The model is constructed based on the papers by Nedley et al (1972) and Riede et al (1984). The basic equations for the vehicle model are:

$$\alpha_f = \frac{u \cdot \beta + a \cdot r}{u} + \delta_s - \delta_{ref} \quad (1)$$

$$\alpha_r = \frac{u \cdot \beta - b \cdot r}{u} - \delta_r \quad (2)$$

$$F_{y1} = -2 \cdot C_{\alpha f} \cdot \alpha_f + 2 \cdot C_{\gamma f} \cdot \gamma_f \quad (3)$$

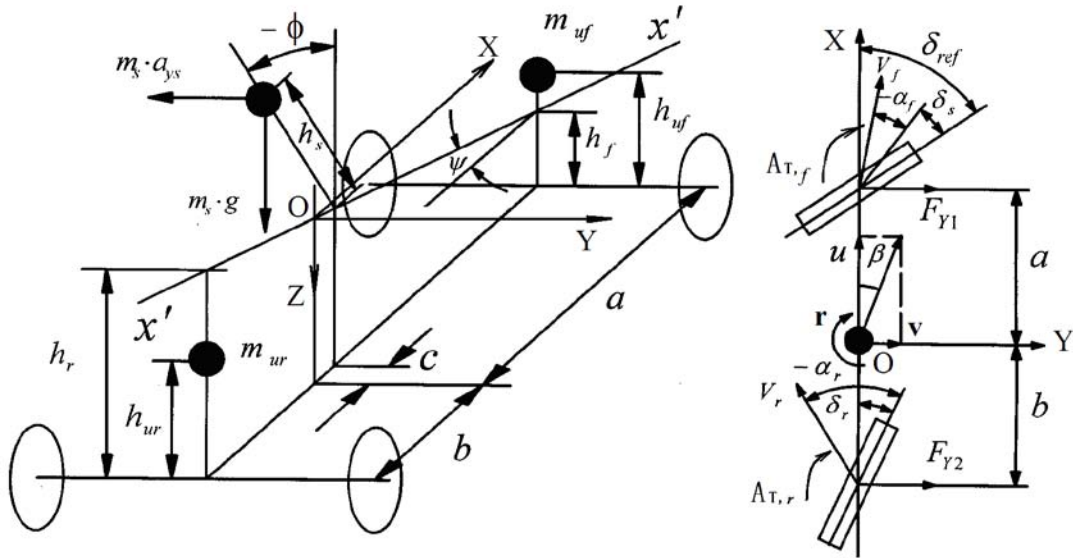


Fig. 2: Linear 3-dof vehicle handling model

$$F_{y2} = -2 \cdot C_{\alpha r} \cdot \alpha_r + 2 \cdot C_{\gamma r} \cdot \gamma_r \quad (4)$$

$$\delta_s = -E_{\varphi f} \cdot \varphi + E_{yf} \cdot \frac{F_{y1} - m_{uf} \cdot (u \cdot \dot{\beta} + a \cdot \dot{r} + u \cdot r)}{2} - E_{nf} \cdot \frac{A_{T,f}}{2} \quad (5)$$

$$A_{T,f} = 2 \cdot N_{\alpha f} \cdot \alpha_f + 2 \cdot N_{\gamma f} \cdot \gamma_f \quad (6)$$

$$\gamma_f = \Gamma_{\varphi f} \cdot \varphi - \Gamma_{yf} \cdot \frac{F_{y1} - m_{uf} \cdot (u \cdot \dot{\beta} + a \cdot \dot{r} + u \cdot r)}{2} + \Gamma_{nf} \cdot \frac{A_{T,f}}{2} \quad (7)$$

$$\delta_r = -E_{\varphi r} \cdot \varphi + E_{yr} \cdot \frac{F_{y2} - m_{ur} \cdot (u \cdot \dot{\beta} - b \cdot \dot{r} + u \cdot r)}{2} - E_{nr} \cdot \frac{A_{T,r}}{2} \quad (8)$$

$$A_{T,r} = 2 \cdot N_{\alpha r} \cdot \alpha_r + 2 \cdot N_{\gamma r} \cdot \gamma_r \quad (9)$$

$$\gamma_r = -\Gamma_{\varphi r} \cdot \varphi + \Gamma_{yr} \cdot \frac{F_{y2} - m_{ur} \cdot (u \cdot \dot{\beta} - b \cdot \dot{r} + u \cdot r)}{2} - \Gamma_{nr} \cdot \frac{A_{T,r}}{2} \quad (10)$$

where, α_f , α_r - front, rear tire slip angle; u - vehicle forward speed; a , b - distance from vehicle center of

gravity to front, rear wheel centerline; δ_s , δ_r - front, rear wheel compliance steer angle; F_{y1} , F_{y2} - front, rear tires

rear tires lateral force; $C_{\alpha f}$, $C_{\alpha r}$ - front, rear tire cornering stiffness; γ_f , γ_r - front, rear tire inclination angle; $C_{\gamma f}$, $C_{\gamma r}$ - front, rear tire camber stiffness; $E_{\phi f}$, $E_{\phi r}$ - front, rear roll steer coefficient; $E_{y f}$, $E_{y r}$ - front, rear lateral force compliance steer coefficient; E_{nf} , E_{nr} - front, rear aligning torque compliance steer coefficient; m_{uf} , m_{ur} - front, rear unsprung mass; $A_{T,f}$, $A_{T,r}$ - front, rear tires aligning torque; $N_{\alpha f}$, $N_{\alpha r}$ - front, rear tire aligning torque stiffness; $N_{\gamma f}$, $N_{\gamma r}$ - front, rear tire aligning torque stiffness due to camber; $\Gamma_{\phi f}$, $\Gamma_{\phi r}$ - front, rear roll camber coefficient; $\Gamma_{y f}$ - front, rear lateral force compliance camber

coefficient; Γ_{nf} , Γ_{nr} - front, rear aligning torque compliance camber coefficient; h_f , h_r - front, rear roll center height; h_{uf} , h_{ur} - front, rear unsprung center of gravity height; m_s - vehicle sprung mass; ψ - roll axis inclination in side view; h_s - distance from sprung center of gravity to roll axis; $K_{\phi f}$, $K_{\phi r}$ - front, rear suspension roll stiffness; $C_{\phi f}$, $C_{\phi r}$ - front, rear suspension roll damping; a_{ys} - lateral acceleration of sprung center of gravity. The equations of motion for the vehicle model are derived as follows, in which ψ is assumed to be zero for simplicity because it's usually small:

$$m_a \cdot (\dot{u} \cdot \dot{\beta} + u \cdot \ddot{r}) + m_s \cdot h_s \cdot \ddot{\phi} = F_{y1} + F_{y2} \quad (11)$$

$$I_z \cdot \ddot{r} - I_{xzs} \cdot \dot{\phi} = a \cdot F_{y1} - b \cdot F_{y2} + A_{T,f} + A_{T,r} \quad (12)$$

$$I_{xs} \cdot \ddot{\phi} - I_{xzs} \cdot \dot{r} + m_s \cdot h_s \cdot u \cdot (\dot{\beta} + \dot{r}) = (m_s \cdot g \cdot h_s - K_{\phi f} - K_{\phi r}) \cdot \phi - (C_{\phi f} + C_{\phi r}) \cdot \dot{\phi} \quad (13)$$

where, m_a - vehicle total mass; I_z - vehicle total yaw inertia; I_{xzs} - sprung roll-yaw product; I_{xs} - sprung roll inertia; g - gravitational acceleration.

Table 1 shows the values of the vehicle model parameters used in the simulation.

Table 1: Values of the vehicle model parameters used in the simulation

$u = 100 \text{ km/h}$ - vehicle forward speed
$C_{\alpha f} = 1608.5 \text{ N/deg}$, $C_{\alpha r} = 1391.4 \text{ N/deg}$ - front, rear tire cornering stiffness
$C_{\gamma f} = 46.3 \text{ N/deg}$, $C_{\gamma r} = 38.8 \text{ N/deg}$ - front, rear tire camber stiffness
$N_{\alpha f} = 45 \text{ Nm/deg}$, $N_{\alpha r} = 32.6 \text{ Nm/deg}$ - front, rear tire aligning torque stiffness
$N_{\gamma f} = 0.0 \text{ Nm/deg}$, $N_{\gamma r} = 0.0 \text{ Nm/deg}$ front, rear tire aligning torque stiffness due to camber
$E_{\phi f} = -0.17 \text{ deg/deg}$, $E_{\phi r} = 0.08 \text{ deg/deg}$ - front, rear roll steer coefficient
$E_{y f} = 0.28 \text{ deg/kN}$, $E_{y r} = -0.01 \text{ deg/kN}$ - front, rear lateral force compliance steer coefficient
$E_{nf} = 1.1 \text{ deg/hNm}$, $E_{nr} = -0.14 \text{ deg/hNm}$ front, rear aligning torque compliance steer coefficient
$\Gamma_{\phi f} = 0.65 \text{ deg/deg}$, $\Gamma_{\phi r} = -0.1 \text{ deg/deg}$ - front, rear roll camber coefficient
$\Gamma_{y f} = 0.25 \text{ deg/kN}$, $\Gamma_{y r} = -0.4 \text{ deg/kN}$ - front, rear lateral force compliance camber coefficient
$\Gamma_{nf} = 0.07 \text{ deg/hNm}$, $\Gamma_{nr} = 0.01 \text{ deg/hNm}$ front, rear aligning torque compliance camber coefficient;
$K_{\phi f} = 1303 \text{ Nm/deg}$, $K_{\phi r} = 730 \text{ Nm/deg}$ - front, rear suspension roll stiffness
$C_{\phi f} = 40 \text{ Nm/(deg/s)}$, $C_{\phi r} = 40 \text{ Nm/(deg/s)}$ - front, rear suspension roll damping
$m_a = 1702 \text{ kg}$ - vehicle total mass
$m_{uf} = 95 \text{ kg}$, $m_{ur} = 132 \text{ kg}$ - front, rear unsprung mass
$m_s = 1475 \text{ kg}$ - vehicle sprung mass
$I_z = 3377.3 \text{ kg-m}^2$ - vehicle total yaw inertia
$I_{xzs} = -28.1 \text{ kg-m}^2$ - sprung roll-yaw product
$I_{xs} = 598.8 \text{ kg-m}^2$ - sprung roll inertia;
$a = 1170.8 \text{ mm}$, $b = 1397.2 \text{ mm}$ distance from vehicle center of gravity to front, rear wheel centerline
$c = 49.6 \text{ mm}$ - distance from sprung center of gravity to vehicle center of gravity
$h_f = 57 \text{ mm}$, $h_r = 194 \text{ mm}$ - front, rear roll center height
$h_{uf} = 305 \text{ mm}$, $h_{ur} = 310 \text{ mm}$ - front, rear unsprung center of gravity height
$h_s = 477 \text{ mm}$ - vehicle total center of gravity height
$h_s = 385.11 \text{ mm}$ - distance from sprung center of gravity to roll axis;

Let

$$Z_\phi = \dot{\phi} \quad (14)$$

$$U = [r, \beta, \phi, Z_\phi]^T \quad (15)$$

$$\dot{\mathbf{U}} = [\dot{r}, \dot{\beta}, \dot{\phi}, \dot{Z}_\phi]^T \quad (16)$$

The equations (11), (12), and (13) can be written in the matrix form with δ_{ref} as the input:

$$\mathbf{M} \cdot \dot{\mathbf{U}} = \mathbf{R} \cdot \mathbf{U} + \mathbf{N} \cdot \delta_{ref} \quad (17)$$

where, \mathbf{M}, \mathbf{R} - 4×4 matrix; \mathbf{N} - 4×1 matrix.

Equation (17) is changed into equation (18) by multiplying \mathbf{M}^{-1} on both sides of it:

$$\dot{\mathbf{U}} = \mathbf{M}^{-1} \cdot \mathbf{R} \cdot \mathbf{U} + \mathbf{M}^{-1} \cdot \mathbf{N} \cdot \delta_{ref} \quad (18)$$

Equation (18) is solved with Runge-Kutta numerical integration method.

In the simulation, the formula of δ_{ref} is

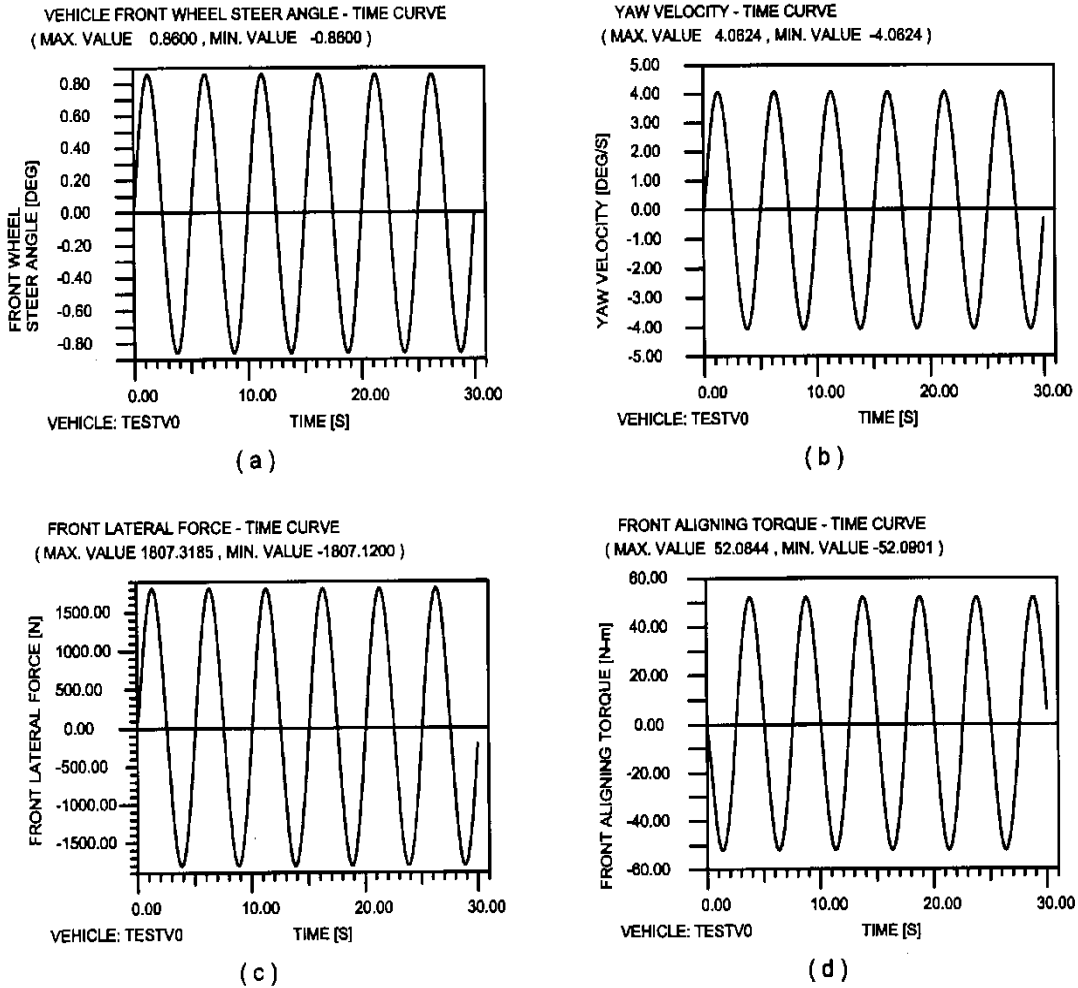


Fig. 3: Input and some response histories of the Linear 3-dof vehicle handling model

In order to obtain the on-center handling characteristics, the steering wheel rotation angle and torque have to be determined. A model of the steering system is constructed to determine them.

$$\delta_{ref} = \delta_{refA} \cdot \sin(2 \cdot \pi \cdot f_H \cdot t) \quad (19)$$

where, δ_{refA} - amplitude of δ_{ref} ; f_H – frequency. Fig.3(a) shows the time history of δ_{ref} in which $\delta_{refA} = 0.86$ deg and $f_H = 0.5$ Hz. Fig.3 (b) shows the corresponding time history of yaw velocity r . And the lateral acceleration a_y is calculated as the product of vehicle speed u and yaw velocity r for easy measurement as prescribed by Norman (1984).

$$a_y = r \cdot u \quad (20)$$

Fig.3(c), (d) show the time histories of F_{y1} , $A_{T,f}$, respectively.

III. MODEL OF THE STEERING SYSTEM

It is assumed that the vehicle studied is a rear drive vehicle equipped with a power integral steering gear and the inertia forces and moments of all parts in the steering system can be neglected. Fig. 4 shows the

model of the steering system. The formula for the kingpin aligning torque $A_{T,K}$ is

$$A_{T,k} = A_{T,f} \cdot \cos \tau \cdot \cos \sigma' - r_d \cdot \sin \tau \cdot \cos \sigma' \cdot F_{y1} - W_f \cdot r_n \cdot \cos \tau \cdot \sin \sigma' \cdot \delta_{ref} \quad (21)$$

$$\sigma' = \operatorname{arctg}(\operatorname{tg} \sigma \cdot \cos \tau) \quad (22)$$

$$r_n = (r_d \cdot \operatorname{tg} \sigma + r_s) \cdot \cos \sigma' \quad (23)$$

where, τ – caster; σ – kingpin inclination angle; r_s – kingpin off-set; r_d – radius of front tire; W_f – vertical load on front axle; camber is assumed to be zero.

Fig. 5 shows the section view of the valve body and valve spool in their assembled position as well as the valve equivalent flow paths.

When the vehicle's engine is running, the flow Q_T from the power steering pump gets into the four axial supply grooves F on the inside diameter of the valve body through the four supply holes E . Then, the flow diverts into two parts, Q_L and Q_R :

- 1) The flow Q_L flows to the left and gets into the four

axial grooves G_{L1} on the outside diameter of the spool through the valve gaps B_1 . This flow again diverts into two parts, Q_B flowing into the power cylinder and $(Q_L - Q_B)$ getting into the four axial grooves G_{L2} on the inside diameter of the valve body through the valve gaps B_2 and further flowing into the center of the spool through the return holes in the spool. The center of the spool is freely communicated to the power steering reservoir and is a low pressure zone.

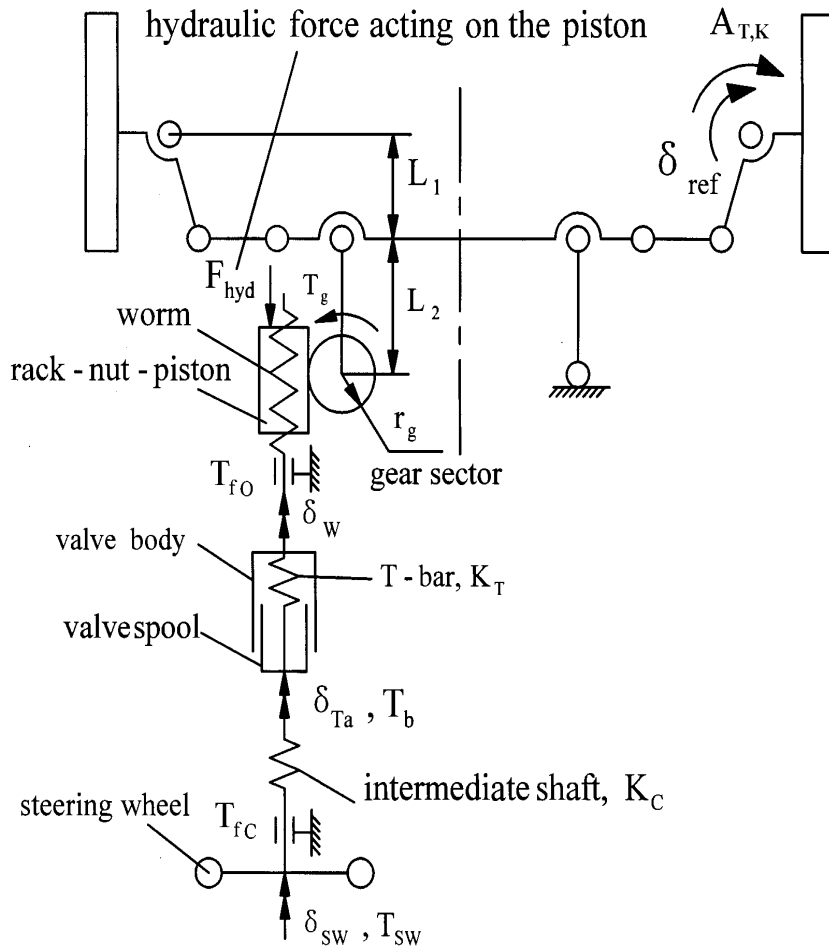


Fig. 4: Model of the integral power steering system

- 2) The flow Q_R flows to the right and gets into the four axial grooves G_{R1} on the outside diameter of the spool through the valve gaps A_1 and is combined with the flow Q_A from the cylinder. The combined

flow $(Q_R + Q_A)$ gets into the four axial grooves G_{R2} on the inside diameter of the valve body through the valve gaps A_2 and further flows into the center of the spool through the return holes in the spool.

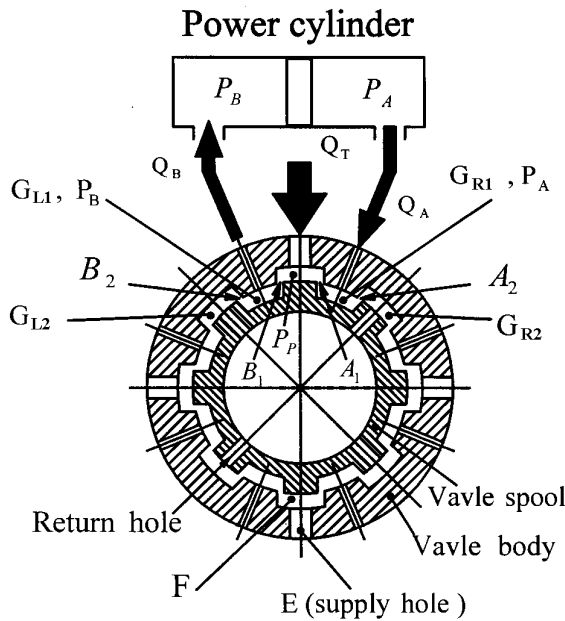


Fig. 5: Section view of the valve body and valve spool in their assembled position as well as the valve equivalent flow paths

The valve spool rotates relative to the valve body as the T-bar (Torsion-bar) is twisted by the torque applied to it, causing the valve gaps A_1 , A_2 , B_1 , and B_2 to change. The basic valve equations are:

$$Q_R = C_q \cdot A_1 \cdot \sqrt{\frac{2 \cdot (P_p - P_A)}{\rho}} \quad (24)$$

$$Q_A + Q_R = C_q \cdot A_2 \cdot \sqrt{\frac{2 \cdot P_A}{\rho}} \quad (25)$$

$$Q_L = C_q \cdot B_1 \cdot \sqrt{\frac{2 \cdot (P_p - P_B)}{\rho}} \quad (26)$$

$$Q_L - Q_B = C_q \cdot B_2 \cdot \sqrt{\frac{2 \cdot P_B}{\rho}} \quad (27)$$

$$Q_T = Q_L + Q_R \quad (28)$$

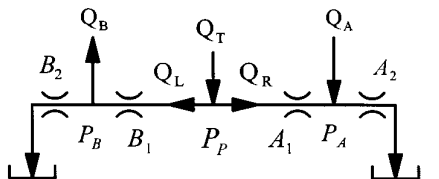
$$Q_A = Q_B \quad (29)$$

where, the pressure at the center of the spool is assumed to be zero; the leakage in the gear is neglected; P_p – pump pressure; P_A , P_B – pressure at the groove G_{R1} , G_{L1} ; C_q – flow coefficient of the valve gaps; ρ – fluid density.

A power integral steering gear was taken apart and its valve geometry was measured. Fig. 6(a) shows the areas of A_1 , A_2 , B_1 , and B_2 versus the rotational angle of the spool relative to the valve body.

Let P_{DIFF} be the pressure differential across the cylinder piston, thus

$$P_{DIFF} = P_B - P_A \quad (30)$$



Valve gap areas : A_1 , A_2 , B_1 , B_2

Fluid flows : Q_T , Q_A , Q_B , Q_L , Q_R

Pressures : P_p , P_A , P_B

Axial grooves: G_{L1} , G_{L2} , G_{R1} , G_{R2} , F

Fig. 6(b) shows the pressure differential P_{DIFF} versus spool rotation angle relative to the valve body. It can be seen that Q_A , Q_B (flows from and to the power cylinder) have effect on P_{DIFF} . P_{DIFF} decreases as Q_A increases and vice versa, with the spool rotation angle kept constant.

Let the ratio of steering linkage be R_{lnk} ,

$$R_{lnk} = \frac{L_1}{L_2} \quad (31)$$

The steering gear applies a torque T_g to balance $A_{T,k}$,

$$T_g = -\frac{A_{T,k}}{R_{lnk}} \quad (32)$$

Let the over-center turning torque of the integral steering gear be T_{fo} when T_g is zero and the steering ratio of the gear be G_R . T_{fo} is assumed to be a dry friction torque. It can be equivalent to a dry friction torque T_{fg} acting on the gear sector,

$$T_{fg} = G_R \cdot T_{fo} \quad (33)$$

The net torque T_{gn} provided by driver's hand and hydraulic assist to the gear sector is

$$T_{gn} = T_g + s_n \cdot T_{fg} \quad (34)$$

$$s_n = \begin{cases} +1 & \text{when } \Delta\delta_{ref} \geq 0 \\ -1 & \text{when } \Delta\delta_{ref} < 0 \end{cases} \quad (35)$$

Let the torsional rate of the T-bar be K_T , its torsional angle be δ_T , and the hydraulic cylinder efficiency be η_{hyd} . When $\Delta\delta_{ref}$ has the same sign as T_{gn} , the torque T_{gn} forces the front wheels to turn. In this case,

$$(K_T \cdot \delta_T) \cdot GR + P_{DIFF} \cdot A_p \cdot r_g \cdot \eta_{hyd} = T_{gn} \quad (36)$$

where, P_{DIFF} - pressure differential across the hydraulic piston; A_p - area of the hydraulic cylinder; r_g -

pitch radius of the gear sector.
The equation (36) can be written as

$$S_{11} \cdot \delta_T + S_{12} \cdot P_{DIFF} = S_{13} \quad (37)$$

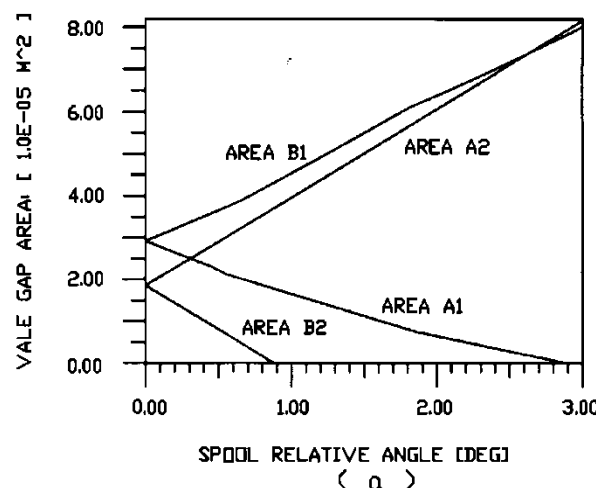
where,

$$S_{11} = K_T \cdot G_R \quad (38)$$

$$S_{12} = A_p \cdot r_g \cdot \eta_{hyd} \quad (39)$$

$$S_{13} = T_{gn} \quad (40)$$

VALVE GAP AREA vs. SPOOL RELATIVE ANGLE CURVE
(MAX. SPOOL RELATIVE ANGLE: 3.0 DEG)



VALVE PRESSURE DIFFERENTIAL vs. SPOOL RELATIVE ANGLE CURVE
(PUMP RELIEF PRESSURE: 10.00 MPa)

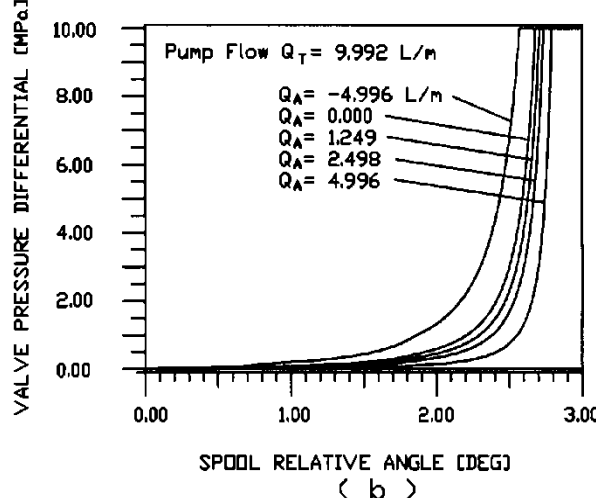


Fig. 6: Valve areas and pressure differential characteristics

When $\Delta\delta_{ref}$ has different sign from T_{gn} , the torque T_{gn} resists the rotation of front wheels. In this case,

$$(K_T \cdot \delta_T) \cdot G_R + P_{DIFF} \cdot A_p \cdot r_g / \eta_{hyd} = T_{gn} \quad (41)$$

The equation (41) can be written as

$$S_{21} \cdot \delta_T + S_{22} \cdot P_{DIFF} = S_{23} \quad (42)$$

where,

$$S_{21} = K_T \cdot G_R \quad (43)$$

$$S_{22} = A_p \cdot r_g / \eta_{hyd} \quad (44)$$

$$S_{23} = T_{gn} \quad (45)$$

So, the equations (37) and (42) can be written as a general form,

$$S_1 \cdot \delta_T + S_2 \cdot P_{DIFF} = S_3 \quad (46)$$

Because δ_T and P_{DIFF} always have the same sign as S_3 , the equation (46) can be written as

$$S_1 \cdot |\delta_T| + S_2 \cdot |P_{DIFF}| = |S_3| \quad (47)$$

$$s_{np} = \begin{cases} +1 & \text{when } V_p \text{ has the same sign as } S_3. \\ -1 & \text{when } V_p \text{ has different sign from } S_3. \end{cases} \quad (51)$$

$$A_p = \frac{\pi \cdot D_p^2}{4} \quad (52)$$

where, D_p - diameter of the power cylinder.

As shown in Fig. 7, the straight line intersects with the pressure differential versus spool rotation angle

$$s_{ns} = \begin{cases} +1 & \text{when } S_3 \geq 0. \\ -1 & \text{when } S_3 < 0. \end{cases} \quad (48)$$

Let $|\delta_T|$ and $|P_{DIFF}|$ be the independent variables, equation (47) is a straight line in Fig. 7, which is obtained by putting the straight line onto Fig. 6(b), the valve pressure differential versus spool relative rotation angle curves.

Let the piston velocity be V_p and the flow to the hydraulic cylinder be Q_A ,

$$V_p = \frac{d(\delta_{ref})}{dt} \cdot R_{lnk} \cdot r_g \quad (49)$$

$$Q_A = s_{np} \cdot |V_p| \cdot A_p \quad (50)$$

curve corresponding to Q_A , giving the solution $|\delta_T|$ and $|P_{DIFF}|$, and

$$\delta_T = s_{ns} \cdot |\delta_T| \quad (53)$$

$$P_{DIFF} = s_{ns} \cdot |P_{DIFF}| \quad (54)$$

**VALVE PRESSURE DIFFERENTIAL VS. SPOOL RELATIVE ANGLE CURVE
(PUMP RELIEF PRESSURE: 10.00 MPa)**

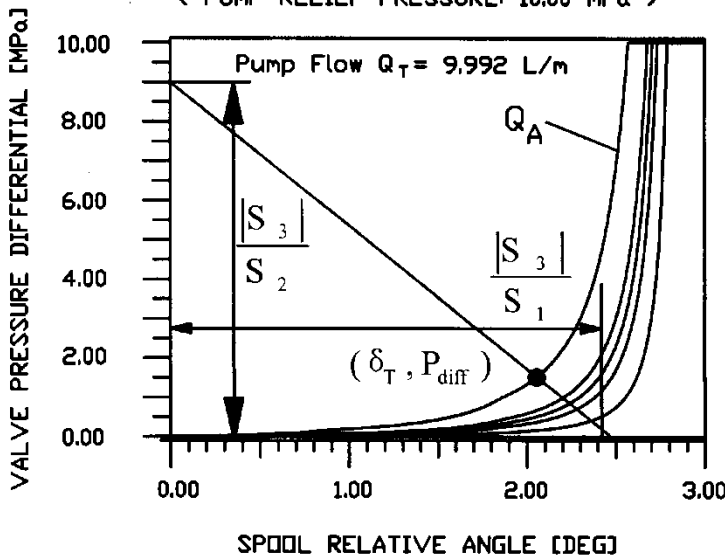


Fig. 7: Model for determining T-bar torsional angle and valve pressure differential

Let the absolute T-bar rotation angle be δ_{Ta} and the T-bar torque be T_b ,

$$\delta_{Ta} = R_{lnk} \cdot \delta_{ref} \cdot G_R + \delta_T \quad (55)$$

$$T_b = K_T \cdot \delta_T \quad (56)$$

Let the torsional rate of the steering intermediate shaft be K_c and the dry friction of the steering column be T_{fc} ,

$$\delta_{sw} = \delta_{Ta} + T_b / K_c \quad (57)$$

$$T_{sw} = T_b + s_{nw} \cdot T_{fc} \quad (58)$$

$$s_{nw} = \begin{cases} +1 & \text{when } \Delta\delta_{sw} \geq 0 \\ -1 & \text{when } \Delta\delta_{sw} < 0. \end{cases} \quad (59)$$

where, δ_{sw} - steering wheel rotation angle; T_{sw} - steering wheel torque.

Table 2 shows the values of the parameters used in the steering system model.

Fig. 8 shows the time histories of pressure differential P_{DIFF} and T-bar torsional angle δ_T . Fig. 9 shows the time histories of δ_{sw} , T_{sw} , and lateral acceleration $a_y(u \cdot r)$.

Table 2: Values of the parameters used in the steering system model

$\tau = 5.0$ deg – caster
$\sigma = 12.0$ deg – kingpin inclination angle
$r_s = 20.0$ mm – kingpin off-set
$r_d = 302.0$ mm – radius of front tire
$W_f = 9260.0$ N – vertical load on front axle
$Q_T = 9.992$ L/m – flow from the power steering pump to the steering gear
$C_q = 0.7$ – flow coefficient of the valve gaps
$\rho = 870$ kg/m ³ - fluid density
$R_{ink} = 0.986$ - ratio of steering linkage
$T_{fo} = 2.2$ Nm - over-center turning torque of the integral steering gear
$G_R = 14.0$ - steering ratio of the integral steering gear
$K_T = 1.2$ Nm/deg - torsional rate of the T-bar
$\eta_{hyd} = 0.8$ - hydraulic cylinder efficiency
D_p - diameter of the hydraulic cylinder
$r_g = 33.33$ mm - pitch radius of the pitman gear sector
$K_c = 0.55$ Nm/deg - torsional rate of the steering intermediate shaft
$T_{fc} = 0.1$ Nm - dry friction of the steering column

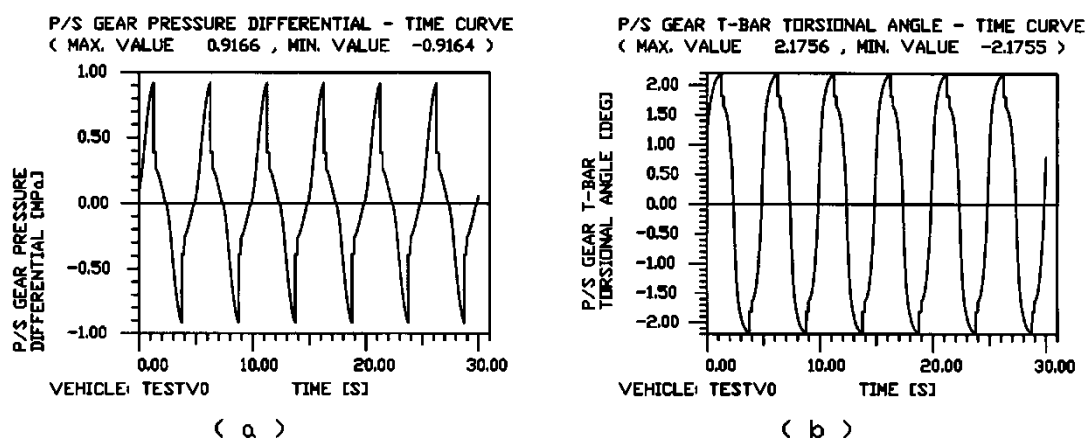


Fig. 8: Time histories of pressure differential P_{DIFF} and T-bar torsional angle δ_T

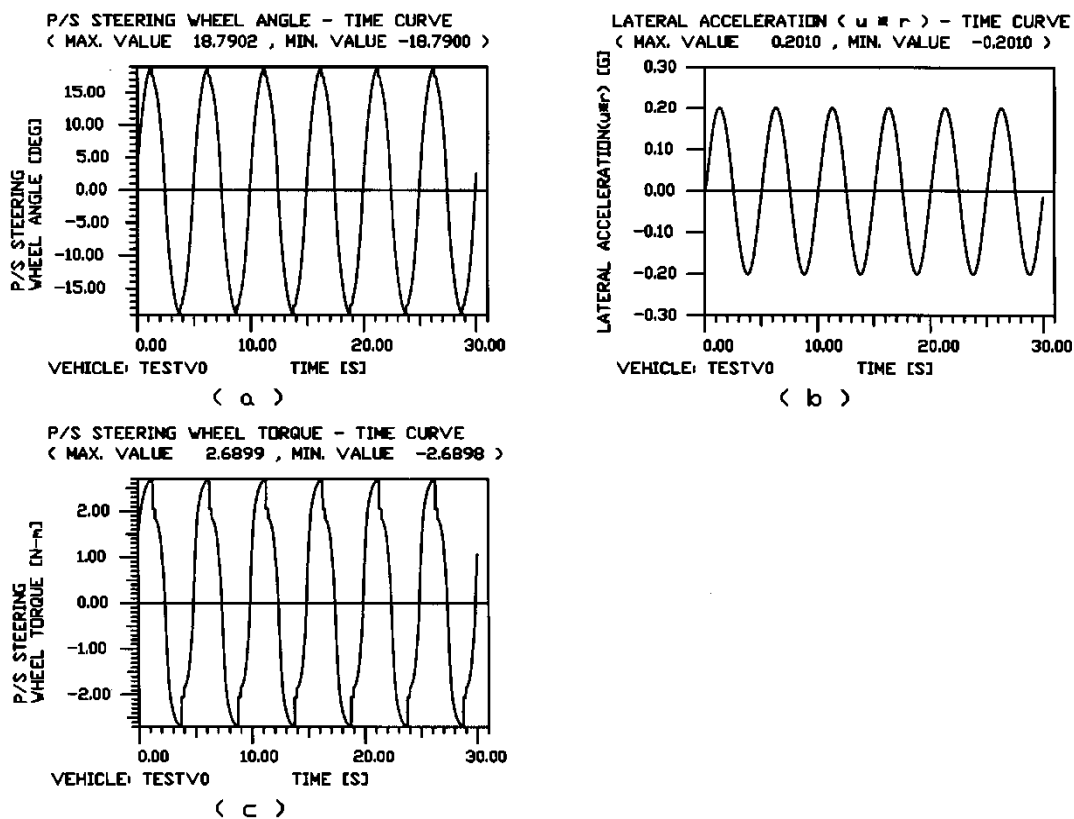


Fig. 9: Time histories of δ_{sw} , T_{sw} , and lateral acceleration $a_y(u \cdot r)$

IV. ON-CENTER HANDLING CROSS-PLOTS AND PARAMETERS

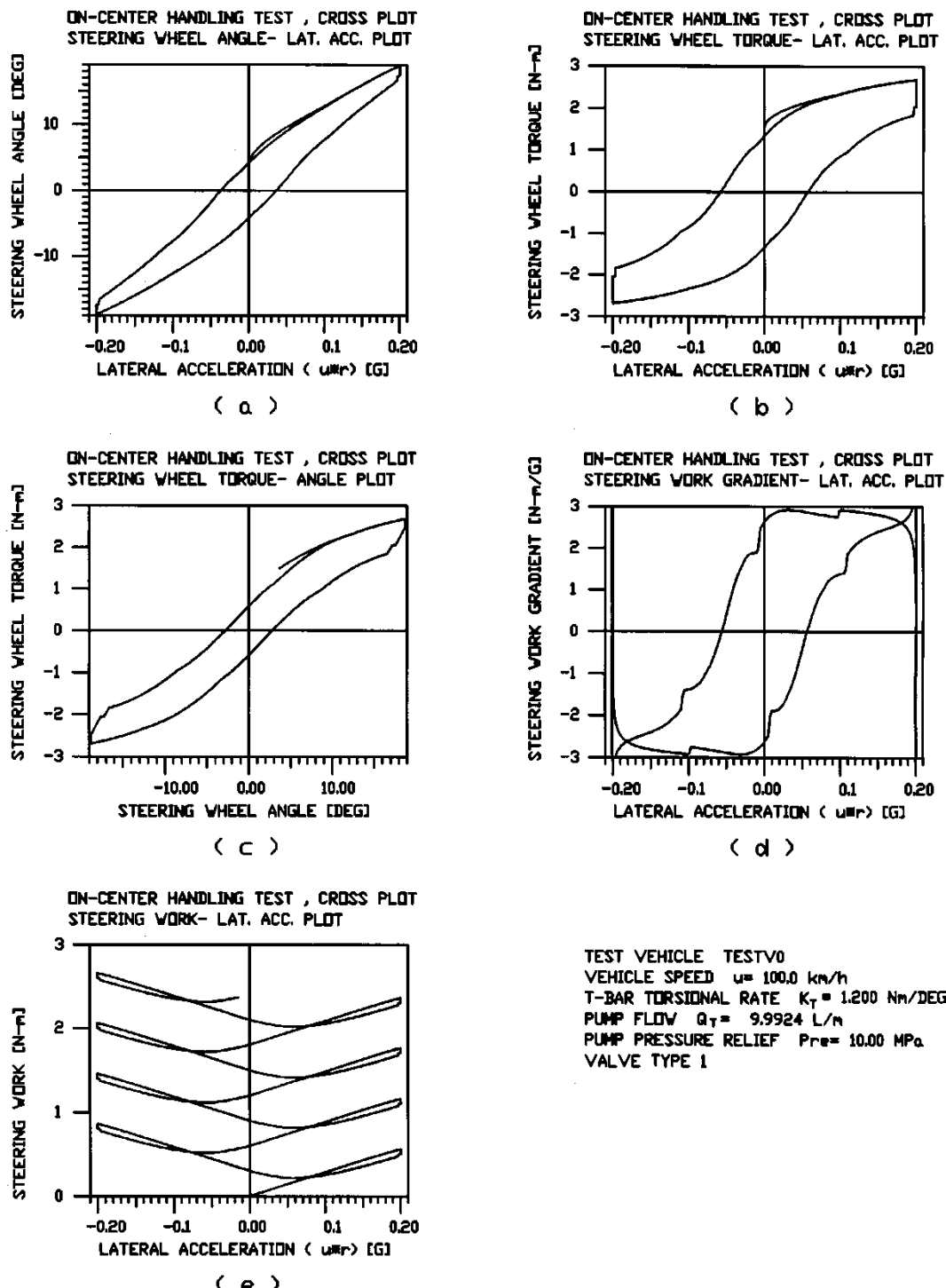
On-center handling cross-plots (as shown in Fig. 10) are drawn from the time histories shown in Fig.

9 and the on-center handling parameters (as shown in Table 3) are obtained from the cross-plots by using the methods described by Norman (1984).

Table 3: Values of the on-center handling parameters obtained by simulation

Steering sensitivity at 0.1g (g's/100deg SW) : 1.40
Minimum steering sensitivity (g's/100deg SW) : 0.72
Steering sensitivity ratio: 0.52
Steering hysteresis (deg SW): 6.95
Steering torque at 0.0g (Nm): 1.34
Steering torque gradient at 0.0g (Nm/g): 20.64
Steering torque at 0.1g (Nm): 2.34
Steering torque gradient at 0.1g (Nm/g): 5.54
Steering torque gradient ratio: 0.27
Lateral acceleration at 0.0Nm (g's): -0.057
Steering torque at 0.0deg SW (Nm): 0.63
Steering torque gradient at 0.0 deg SW (Nm/deg): 0.21
Steering work sensitivity (g ² /100Nm): 4.3

Compared with the data provided by Norman (1984) and Kunkel et al (1988), the simulation results as shown in Table 3 are reasonable.

Fig. 10: On-center handling cross-plots ($Q_T = 9.992 \text{ L/m}$)

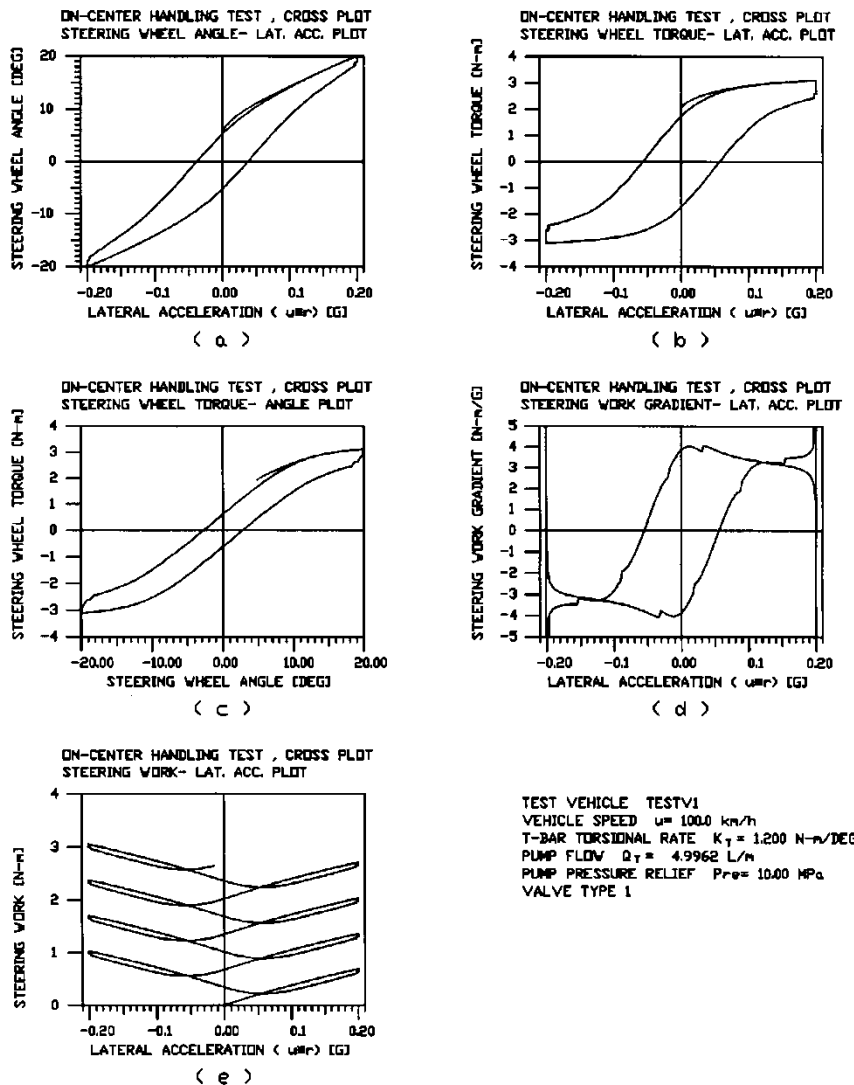
The effects of changing the values of the vehicle and its steering system parameters on the on-center handling characteristics can be studied with the simulation, which helps to find the appropriate system parameters combination to make a car have good on-center handling characteristics. For example, if only Q_T (flow from the power steering pump to the steering gear) is changed from 9.992 L/m to 4.996 L/m, with all other

parameters kept unchanged, in the above simulation, the new simulation results are shown in Fig. 11 and Table 4. The steering torque gradient at 0.0g are changed from 20.64 (Nm/g) to 26.3 (Nm/g) and steering work sensitivity from 4.3(g²/100Nm) to 3.1(g²/100Nm), which are got improved.

Table 4: New values of the on-center handling parameters obtained by simulation *

Steering sensitivity at 0.1g (g's/100deg SW) : 1.50
 Minimum steering sensitivity (g's/100deg SW) : 0.67
 Steering sensitivity ratio: 0.44
 Steering hysteresis (deg SW): 8.34
 Steering torque at 0.0g (Nm): 1.74
 Steering torque gradient at 0.0g (Nm/g): 26.03
 Steering torque at 0.1g (Nm): 2.91
 Steering torque gradient at 0.1g (Nm/g): 3.77
 Steering torque gradient ratio: 0.15
 Lateral acceleration at 0.0Nm (g's): -0.055
 Steering torque at 0.0deg SW (Nm): 0.63
 Steering torque gradient at 0.0 deg SW (Nm/deg): 0.22
 Steering work sensitivity (g²/100Nm): 3.1

* Compared with the simulation in the Table 3, only the flow from the power steering pump to the steering gear Q_T is changed from 9.992 L/m to 4.996 L/m, with all other parameters kept unchanged.

**Fig. 11:** On-center handling cross-plots ($Q_T = 4.996 \text{ L/m}$)

V. CONCLUSION

In the simulation of on-center handling test, a simple linear 3-dof (degrees of freedom) vehicle handling model and a comprehensive power integral steering system model are incorporated to calculate the time histories of steering wheel angle, steering wheel torque, and vehicle lateral acceleration, from which the on-center handling cross-plots and parameters are obtained. The linear 3-dof vehicle handling model can give sufficiently accurate simulation results in the lateral acceleration range (peak value is about 0.2g) of the on-center handling tests. Because the rotation angle amplitude and frequency of the steering wheel are small, the inertia forces and moments of all parts in the steering system can be neglected, which makes the steering system model much simpler. Compared with the data presented in the literatures, the simulation results obtained are reasonable. So the simulation can be useful in finding the appropriate system parameters combination to make a car have good on-center handling characteristics.

REFERENCES RÉFÉRENCES REFERENCIAS

1. Norman, K. D. (1984) 'Objective evaluation of on-center handling performance', SAE technical paper, No. 840069, pp.1~13.
2. Post, J. W. and Law, E. H. (1996) 'Modeling, characterization and simulation of automotive power steering systems for the prediction of on-center handling', SAE technical paper, No. 960178, pp.1~10.
3. Kim, H. S. (1997) 'The investigation of design parameters influencing on on-center handling using AUTOSIM ', SAE technical paper, No. 970102, pp.1~10.
4. Nedley, A. L. and Wilson, W. J. (1972) 'A new laboratory facility for measuring vehicle parameters affecting under steer and brake steer', SAE technical paper, No. 720473, pp.1~19.
5. Riede, P. M., Leffert, R. L. and Cobb, W. A. (1984) 'Typical vehicle parameters for dynamics studies revised for the 1980's', SAE technical paper, No. 840561, pp.1~15.
6. Kunkel, D. T. and Leffert, R. L. (1988) 'Objective directional response testing', SAE technical paper, No. 885008, pp.1~15.



This page is intentionally left blank